

Investigation of Influencing Factors on Power Generation Performance in Reverse Electrodialysis

Aydın CİHANOĞLU^{1,2*}

¹Department of Chemical Engineering, Faculty of Engineering, Ege University, İzmir, 35100, Türkiye

²Refinery and Petrochemical Technology, Aliğa Vocational School, Ege University, İzmir, 35800, Türkiye

Received: 04/11/2024, **Revised:** 15/12/2024, **Accepted:** 23/12/2024, **Published:** 31/12/2024

Abstract

The importance of meeting energy demands from renewable sources is growing daily. Reverse electrodialysis (RED) is a membrane-based technology that produces energy using electrolyte solutions with different salinities. This study has generated energy from the RED system using the commercial Fujifilm Type II ion exchange membranes (IEMs). Many parameters affect the power generation performance of the RED system. This study systematically investigated the parameters, the presence of divalent ions and organic molecules, the electrolyte solution concentration, and the flow velocity. The flow velocity results indicated that energy efficiency increased with increasing flow velocity of the electrolyte solutions. The presence of divalent ions created uphill transport. The results showed that increasing the mole ratio of divalent ions in the feed electrolyte solutions dramatically decreased the RED system performance due to increasing resistances. The organic fouling test of the anion exchange membranes (AEMs) was carried out using a real humic and fulvic acid mixture under static conditions. The results indicated that fouling layers formed in the AEMs structure, and these layers decreased by 30% of RED performance. Lastly, the RED system's long-term performance was tested for 4 hours at a constant current density of 8 A/m² before and after AEM fouling experiments. The results revealed the fouling layers severely reduced the power generation performance of the RED system.

Keywords: reverse electrodialysis, ion exchange membrane, uphill transport, organic fouling, blue energy.

Ters Elektrodializde Güç Üretim Performansını Etkileyen Faktörlerin Araştırılması

Öz

Enerji taleplerini yenilenebilir kaynaklardan karşılamının önemi her geçen gün artmaktadır. Ters elektrodializ (RED), farklı tuzluluklara sahip elektrolit çözeltileri kullanarak enerji üreten membran tabanlı bir teknolojidir. Bu çalışmada ticari Fujifilm Tip II iyon değiştirici membranlar (IEMs) kullanılarak RED sisteminden enerji üretilmiştir. RED sisteminin güç üretim performansını birçok parametre etkilemektedir. Bu çalışmada, iki değerlikli iyonların ve organik moleküllerin varlığı, elektrolit çözelti konsantrasyonu ve akış hızı sistematik olarak araştırılmıştır. Akış hızı sonuçları, elektrolit çözeltilerinin akış hızının artmasıyla enerji verimliliğinin arttığını göstermiştir. Çift değerlikli iyonların varlığı konsantrasyon gradyanının tersine taşınım yarattı. Sonuçlar, besleme elektrolit çözeltilerindeki iki değerlikli iyonların mol oranının artırılmasının, artan dirençler nedeniyle RED sistem performansını önemli ölçüde azalttığını gösterdi. Anyon değiştirici membranların (AEMs) organik kirlenme testi, statik koşullar altında gerçek hümik ve fulvik asit karışımı kullanılarak gerçekleştirildi. Sonuçlar, AEM yapısında kirlenme tabakalarının oluştuğunu ve bu tabakaların RED performansını %30 oranında azalttığını gösterdi. Son olarak, RED sisteminin uzun vadeli performansı, AEM kirlenme deneylerinden önce ve sonra 8 A/m² sabit akım yoğunluğunda 4 saat boyunca test edildi. Sonuçlar, kirlenme katmanlarının RED sisteminin güç üretim performansını ciddi şekilde azalttığını ortaya koydu.

Anahtar Kelimeler: ters elektrodializ, iyon değiştirici membran, konsantrasyon gradyanı tersine taşınım, organik kirlilik, mavi enerji.

1. Introduction

Access to energy is one of the most fundamental human rights required to improve people's living standards and ensure sustainability. The meeting energy demand of the rapidly growing population with fossil fuels is a huge problem for all living due to its hazardous impact on the environment. Salinity gradient energy (SGE), also called blue energy, is considered a promising technology since its efficiency and sustainability are not dependent on external conditions, and it does not produce solid, liquid, or gas waste. This technology produces energy by converting chemical potential into electrical or mechanical energy [1-4]. The potential source of this technology is the sea and river water and the place where the junction of these two sources. Theoretical studies based on Gibbs's free energy calculations report that the global potential of SGE considering entire regions that could be used is around 1.4-2.6 TW. This is equivalent to 20% of total demand [2,3,5]. Using the full potential of SGE could reduce energy-related CO₂, CH₄, and N₂O emissions by 25%, 27%, and 8% respectively [6]. The SGE technology includes three different techniques, RED, PRO (pressure retarded osmosis), and CapMix (capacitive mixing) [1]. Of the mentioned techniques, RED is considered the most promising of those proposed so far because of its high power density and functionality [7-9]. Technically, a RED stack consists of AEMs and CEMs (cation exchange membranes) placed in succession between electrodes, and a spacer and gasket separate these membranes. The concentrate and dilute electrolyte solutions are fed to compartments between IEMs. The salinity difference across IEMs creates a Nernst potential, and this potential is converted to electricity by a redox reaction at electrodes.

Many researchers have been working on renewable energy harvesting from the RED system using standard commercial IEMs and NaCl salt ions [10-12]. Further, the effect of membrane type [11,12], flow rate [13,14], spacer thickness [15], electrode system [16-18], and feed concentration [19] on power generation was comprehensively investigated. However, few studies are focused on the effect of multivalent ions and organic substances on power generation performance. The studies in the literature that used NaCl do not accurately shed the actual industrial-scale RED energy harvesting performance because the electrolyte solutions in the actual applications do not include only monovalent ions. The multivalent ions decrease the power generation, depending on the concentration in the feed electrolyte solutions. The reason for performance loss is the uphill transport that occurs in the presence of multivalent ions, creating high resistance in the RED system. In this transport, multivalent ions are transported against the concentration gradient, whereas monovalent ions are transported through the concentration gradient. This counter-current transport of ions creates electroneutrality, resulting in potential differences reduction between the compartments and a loss of power density by increasing the resistance [20]. For instance, Vermaas et al. reported that almost 50% loss of power density in the RED system, where Fujifilm IEMs were located, was obtained when the 10% MgSO₄ and 90% NaCl of mole fraction were in the feed electrolyte solution in both concentrate and dilute compartments [21]. Similarly, Pintossi et al. studied the effect of multivalent ions on the RED performance using commercial FujiFilm IEMs. They concluded the presence of multivalent ions increases the resistance of the RED system and decreases the permselectivity of the IEMs [22]. Organic fouling is another problem in power generation from

the RED system on an industrial scale. The presence of organic substances, a source of fouling, creates a fouling layer in the membrane structure, reducing the power generation performance by increasing resistance and decreasing the permselectivity of the IEMs. For instance, the first laboratory-scale RED fouling test results, using sea and river water as the electrolyte solution, showed a high-pressure drop during operation even though pretreatment was applied to the feed solutions with a 20-micron filter [23]. This was attributed to organic fouling layer formation, especially in the AEMs structure.

This work aims to systematically study four fundamental parameters that affect the power generation performance of the RED system using commercial Fujifilm IEMs. These parameters are i) the flow velocity of electrolyte solutions, ii) electrolyte solution concentrations, iii) the presence of divalent ions, and iv) the presence of organic acids. To this end, three different flow velocities and two different electrolyte solution concentrations were used. The effect of divalent ions was first investigated using the same concentration in concentrate and dilute compartments. Then, the compartment composition effect was studied by changing the divalent ion concentrations in the compartments. The organic fouling tendency of AEMs was tested using a real humic and fulvic acid mixture solution under static conditions. The long-term energy generation performance of the RED system was determined before and after the organic fouling test of AEMs.

2. Material and Methods

2.1. Materials and chemicals

This study used commercially available AEMs (Fujifilm Type II) and CEMs (Fujifilm Type II) from Fujifilm manufacturers as ion exchange membranes (IEMs). IEMs were washed with deionized water and stored in 0.5 M NaCl solution for at least one day before use. The properties of IEMs are given in Table 1. Analytical grade $K_3Fe(CN)_6$, $K_4Fe(CN)_6$, and NaCl were used to prepare the electrode solution and NaCl and Na_2SO_4 for electrolyte solutions. All chemicals used in electrode and electrolyte solutions preparations were supplied from Merck (Germany) and used without further purification. The real (not model) humic and fulvic acid mixture (Ant, Türkiye) was used for the fouling test. All solutions were prepared with deionized water.

2.2. Experimental set-up

A schematic view of the RED system (STT Products B.V. BA Schiedam, Netherlands) is given in Figure 1. The electrodes in the system are Ti/Ru-Ir alloyed mesh-type anode and cathode. The polyamide 6-based spacers (Sefar, Switzerland) with 450-micron thickness, 71% porosity, and 38% open areas and silicon rubber gasket were used to separate the membranes with a 10cm x 10cm active area in the RED system [24]. Three repeat units (one repeat unit consisting of one AEM and one CEM) were used in the study. Dilute and concentrate solutions were represented as low and high salinity, respectively. The electrode solution was fed as a closed loop circulated to the electrodes. Two peristaltic pumps were operated for the dilute, concentrate, and electrode solutions feeding speed adjustment in the RED system. The feeding speed of the electrolyte solutions was changed during the study, but the electrode feeding speed

was constant at a 300 mL/min volumetric flow rate. Electrochemical measurements were carried out using Gamry Instrument Reference 3000 (USA). All RED tests were carried out at room temperature (25 °C). RED test experiments were repeated four times, and the standard deviations of the power were obtained on the order of 10^{-4} . Since the standard deviation values were too small, they did not add to the values.

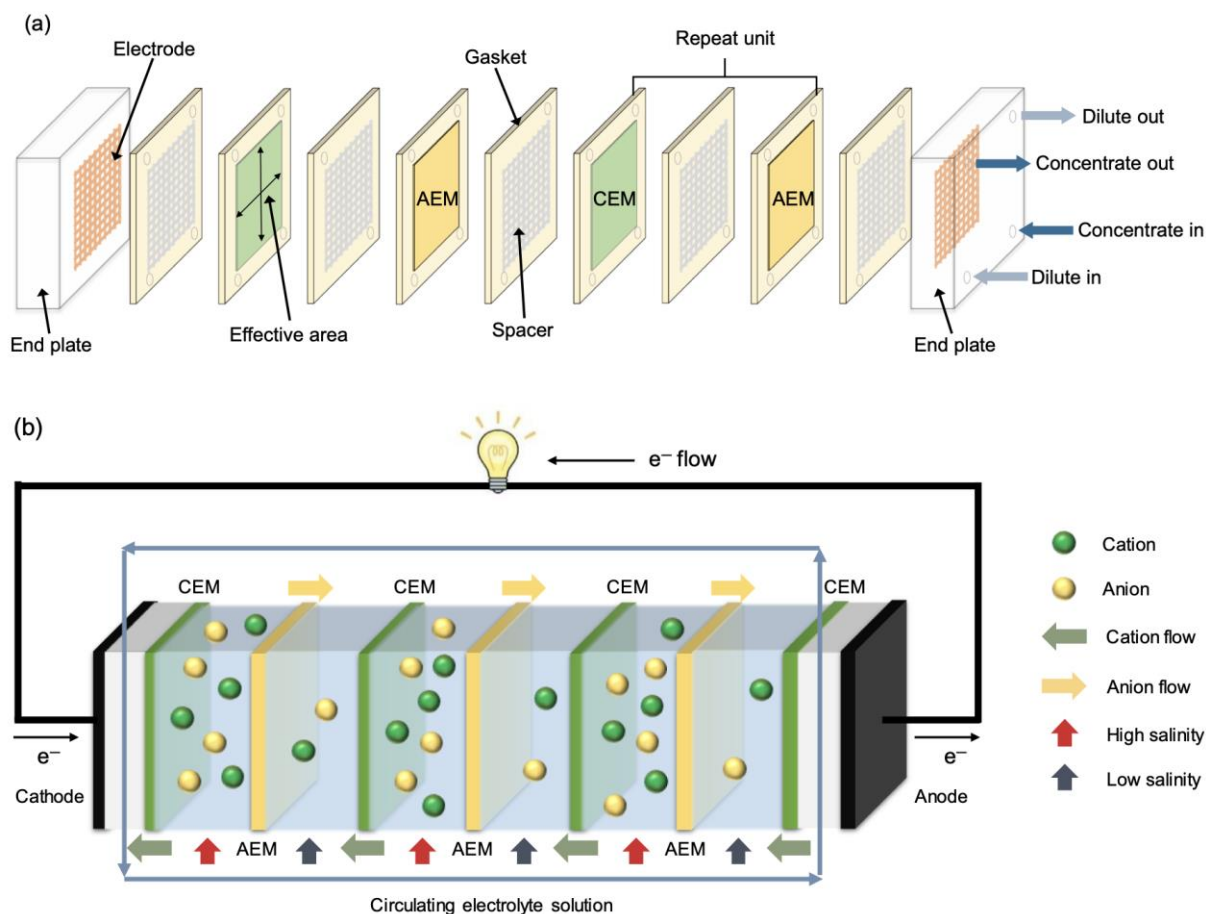


Figure 1. A schematic view of the RED system, a) components, and b) working principle. The figure is reprinted with permission from [25] (Copyright 2020, Elsevier).

2.3. Electrode and electrolyte solution preparation

The electrode solution (2 L) was prepared using 0.05 M $K_3Fe(CN)_6$, 0.05 M $K_4Fe(CN)_6$, and 0.25 M NaCl ions. To this end, all chemicals were well mixed using deionized water at room temperature (25 °C). Then, the mixture was put in a sunlight-proof tank for use. Two different electrolyte solutions, dilute and concentrate, are used in the RED system. The 0.017 M NaCl (dilute) / 0.513 M NaCl (concentrate) solution pair and 0.1 M NaCl (dilute) / 2.5 M NaCl (concentrate) solution pair were separately used as electrolyte solution pairs. On the other hand, in the experiments where monovalent (NaCl) and multivalent ions (Na_2SO_4) were present simultaneously, only a 0.017 M NaCl / 0.513 M NaCl solution pair was used. The Na_2SO_4 concentration was adjusted to be 10% and 50% mole of the total solution concentration. Multivalent ions were added to both dilute and concentrate electrolyte solution compartments.

The label was coded as 90% NaCl+10% Na₂SO₄ and 50% NaCl+50% Na₂SO₄ for 10% and 50% mole ratios, respectively.

2.4. Theoretical background

The salinity difference between the compartments creates a potential difference known as the Nernst potential. The theoretical open circuit voltage (OCV) (V) (when no current is allowed) of each compartment in the presence of monovalent and multivalent ions is calculated using Equations 1 and 2, respectively [26].

$$OCV_{theoric} = \left(\frac{\alpha_{AEM}}{z_-} + \frac{\alpha_{CEM}}{z_+} \right) * \frac{RT}{F} * \ln \left(\frac{m_c \gamma_c}{m_d \gamma_d} \right) \quad (1)$$

$$OCV_{theoric} = \left[\left(\frac{\alpha_{CEM}}{z_{Na^+}} \right) * \frac{RT}{F} * \ln \left(\frac{m_c^{Na^+} \gamma_c^{Na^+}}{m_d^{Na^+} \gamma_d^{Na^+}} \right) \right] + \left[\left(\alpha_{AEM} \right) * \frac{RT}{F} * \left[\frac{1}{z_{Cl^-}} * \ln \left(\frac{m_c^{Cl^-} \gamma_c^{Cl^-}}{m_d^{Cl^-} \gamma_d^{Cl^-}} \right) + \frac{1}{z_{SO_4^{2-}}} \ln \left(\frac{m_c^{SO_4^{2-}} \gamma_c^{SO_4^{2-}}}{m_d^{SO_4^{2-}} \gamma_d^{SO_4^{2-}}} \right)^{1/2} \right] \right] \quad (2)$$

α_{AEM} and α_{CEM} are the membrane permselectivity, z_- , and z_+ are the negative and positive ion valence, respectively, R is the universal gas constant (8.31 J/mol K), T is the temperature (K), F is the Faraday constant (96485 C/mol), m is the molality of the electrolyte solution, γ is the activity coefficient of the ion. The subscripts c and d of constants in the equations represent the concentrated and dilute compartments.

The maximum net power density (P_{Net}) (W/m²) is calculated as the difference in power densities created by the RED system and consumed by the pumps (P_{Pump}). Equations 3-8 are used for the calculations of P_{Net} [27,28].

$$P_{Net} = \frac{(OCV)^2}{4 R_{Cell}} - P_{Pump} \quad (3)$$

$$P_{Pump} = \frac{\sum \Delta P_i * \phi_i}{A_{Membrane}} = \frac{\Delta P_c * \phi_c + \Delta P_d * \phi_d}{A_{Membrane}} \quad (4)$$

$$\Delta P = \frac{12 * \mu * L^2}{\left(\frac{1}{4} \right) * d_h^2 * t_{res}} \quad (5)$$

$$d_h = \frac{4 * \varepsilon}{\left(\frac{2}{h} \right) + (1 - \varepsilon) * \left(\frac{8}{h} \right)} \quad (6)$$

$$t_{res} = \frac{L}{U} \quad (7)$$

$$U = \frac{\phi}{w * h * \varepsilon * N} \quad (8)$$

R_{Cell} is the total resistance of the RED stack ($\Omega \text{ cm}^2$), ΔP is the pressure difference over the feed water compartment (Pa), Φ volumetric flow rate (m³/s), $A_{Membrane}$ is the total membrane area (m²), μ is the viscosity of the electrolyte solution (Pa s), L is the cell length (m), d_h is the hydraulic diameter of the channel (m), t_{res} is the residence time of the electrolyte solution in the

RED stack (s), ε is the porosity of the spacer, h is the intermembrane distance (m), U is the linear flow velocity (m/s), w is the membrane width (m) and N is the membrane number.

The flow regime (Reynolds number, Re) of electrolyte solutions is determined by Equation 9.

$$Re = \frac{2*\phi*\rho}{w*\mu*\varepsilon} \quad (9)$$

ρ is the electrolyte solution density (kg/m³).

Table 1. Properties of Fujifilm Type II IEMs used in the RED stack [29].

Properties	AEM	CEM
Reinforcement	Polyolefin	Polyolefin
Thickness dry (μm)	160	160
Electrical resistance (Ω cm ²)	5	8
Perm selectivity (%)	95	96
Ion exchange capacity (meg/g)	0.9	1.1
pH stability	2-10	4-12
Temperature stability (°C)	40	40

2.5. Fouling test

The fouling tendency of the commercial AEMs was tested in the presence of a real (not model) humic and fulvic acid mixture (Ant, Türkiye). The humic and fulvic acid mixture is an organic acid, and it is commonly present in sea and river water. To this end, the membranes were immersed in the solution with a 20-ppm acid mixture under static conditions for 7 days at room temperature (25 °C). Then, membranes were washed with deionized water to desorb weakly adsorbed organic molecules in the membrane structure. After simple rinsing, the power generation performance of the fouled membranes in the RED system was tested using a 0.017 M NaCl / 0.513 M NaCl electrolyte solution pair under a constant flow velocity of 0.52 cm/s at room temperature (25 °C).

2.6. Long-term test

The long-term power generation performance of IEMs was tested before and after fouling experiments using a constant current density of 8 A/m² and a flow velocity of 0.52 cm/s with a 0.017 M NaCl / 0.513 M NaCl electrolyte solution pair. The experiments took 4 hours and were at room temperature (25 °C). The current density that achieved the highest power density has been identified as the optimum current density value used in long-term performance tests.

Table 2 summarizes the experimental conditions and parameters used in the energy generation performance in the reverse electrodialysis system.

Table 2. Experimental conditions for energy generation from the RED stack.

Membranes	The electrolyte solution concentration	Flow velocity (cm/s)	T (°C)	Presence of divalent ions (moles %)	Presence of organic compound (ppm)*
Fujifilm Type II AEM & CEM	0.017 M NaCl & 0.513 M NaCl	0.26	25	10% Na ₂ SO ₄	20
		0.52		50% Na ₂ SO ₄	
Fujifilm Type II AEM & CEM	0.1 M NaCl & 2.5 M NaCl	2.09		-	-

* The effect of organic compound presence on energy generation performance was tested only using 0.017 M NaCl & 0.513 M NaCl electrolyte solution concentration with 0.52 cm/s solution velocity conditions.

3. Results and Discussion

In this study, the RED performance of the commercially available Fujifilm Type II IEMs was tested using different electrolyte solution concentrations, flow velocities, the presence of multivalent ions, and organic foulants. The effect of these four variables on the RED system performance is crucial. The power generation performance is based on creating a maximum potential difference between the compartments by transporting the ions from the concentrate to dilute compartments and a minimum total resistance during the operation. The theoretical OCV in Equations 1 and 2 indicate that the solution concentration is the most significant parameter since it influences the created potential difference logarithmically [26]. On the other hand, the resistances in the RED system consist of ohmic and non-ohmic. Membrane resistance, spacer properties, electrolyte solution conductivity, inter-membrane distance, and electrode resistance are significant parameters in determining the ohmic resistances. The non-ohmic resistances are based on two fundamental phenomena: boundary layer area resistance and area resistance due to bulk concentration changes. The flow velocity of the electrolyte solution is one of the most significant parameters, reducing these two resistances by decreasing concentration polarization on the membrane surface [13].

In real applications, the feed electrolyte solutions include multivalent ions and organic molecules that trigger the membrane fouling, reducing the power generation performance [23]. The presence of multivalent ions causes uphill transport. In this transport, three scenarios negatively affect the RED system performance: i) transport of multivalent ions from the dilute to concentrate compartments, ii) binding the multivalent ions to a single fixed-charged group, iii) binding the multivalent ions to multiple fixed-charged groups in the membrane structure. In the first scenario, the transport of multivalent ions creates electroneutrality by dropping the potential difference between the compartments because two monovalent ions (Cl⁻) are equal to one divalent ion (SO₄²⁻) in the opposite transport direction. In the second scenario, a multivalent ion stack inside the membrane cross-section structure decreases the ion exchange capacity and permselectivity. In the third scenario, multivalent ions located within the membrane cross-

section cause severe membrane resistances since they reduce the free volume of the membrane, resulting in the reduction of the ion exchange capacity. [20-22]. Lastly, organic molecules in the feed solution create fouling layers in the membrane structure, and the layers prevent ion transport by increasing membrane resistance. These layers also cause an increased pressure drop, increasing the pumping power of the electrolyte solution to the RED system. Therefore, the P_{Net} produced by the RED system is reduced by increased energy consumption [27]. This study investigated the effects of the parameters above-mentioned on power generation performance in detail.

3.1. Effect of concentration and flow velocity of electrolyte solution on RED performance

Table 3 indicates the power generation performance, where only NaCl salt ions were used. The power density values in Table 3 are the maximum values obtained from the RED system. The maximum power density was obtained at a current density of 4 A/m² for the 0.017 M NaCl / 0.513 M NaCl electrolyte solution pair while at a current density of 6 A/m² for the 0.1 M NaCl / 2.5 M NaCl electrolyte solution pair. The results indicated that the power density increased with increasing flow velocity at both concentration pairs. Similarly, the same trend in the effect of flow velocity and feed electrolyte concentration on power generation performance was observed in the literature [7, 29]. Increasing the flow velocity allows for decreasing the non-ohmic resistances formed in the membrane structure [13]. The thickness of the boundary and bulk concentration layers, known as non-ohmic resistances, increase on the membrane surface on time, especially at low flow velocities, and create a mass transfer resistance [28]. Decreasing t_{res} (Equation 7) and increasing Re (Equation 9) cause the acceleration of ion transport across the membrane cross-section, increasing the generated power density since boundary and bulk concentration layer thicknesses decrease. Similarly to the power density values, the experimental OCV and calculated average membrane permselectivity (%) values shown in Figure 2 also increase as the flow velocity increases due to decreasing non-ohmic resistances.

Further, Table 3 points out no significant difference in power density between the solution pairs with different salinities at flow velocities of 0.26 cm/s and 0.52 cm/s, even though there was a statistical difference in the theoretical and experimental OCV values at these velocities between the solution pairs. However, the generated power density at the flow velocity of 2.09 cm/s in the 0.017 M NaCl / 0.513 M NaCl electrolyte solution pair was higher than the 0.1 M NaCl / 2.5 M NaCl electrolyte solution pair. This result is consistent with the OCV and permeability in Figure 2.

It is known that the power density produced by the RED system also includes the P_{Pump} . Therefore, calculating the P_{Net} produced by the system is extremely important in determining the system's efficiency. Table 3 shows the highest power density value was obtained at a 2.09 cm/s flow velocity in both electrolyte solution pairs. In parallel with this result, the power consumed by the pump at the highest flow velocity was also calculated as the highest. At this point, although the RED system produced the highest power value at a flow velocity of 2.09 cm/s, considering the P_{Pump} , it was found that the P_{Net} generated at a flow velocity of 0.52 cm/s was the optimum value for the RED system. Also, the system yield calculations show that the highest efficiency was achieved at a flow velocity of 0.52 cm/s for both solution pairs.

Investigation of Influencing Factors on Power Generation Performance in Reverse Electrodialysis

Considering the results in this section, 0.017 M NaCl / 0.513 M NaCl electrolyte solution pair was selected as the optimum for the remainder of the studies due to the higher yield obtained from the RED system. This choice also serves the idea of using the RED system in real applications at the junction of sea (0.513 M NaCl) and river (0.017 M NaCl) on a model scale.

Table 3. The RED performance of Fujifilm Type II IEMs in the presence of monovalent ions.

Feed Compositions	Flow velocity (cm/s)	Re	t_{res} (s)	Power density (W/m ²)	P _{Pump} (W/m ²)	P _{Net} (W/m ²)	*P _{Theoric} (W/m ²)	**Yield (%)
0.017M (NaCl) & 0.513M (NaCl)	0.26	2.30	38.4	0.156	0.001	0.155	0.270	57.4
	0.52	4.70	19.1	0.175	0.004	0.171		63.3
	2.09	18.7	4.80	0.197	0.066	0.131		48.5
0.1 M (NaCl) & 2.5 M (NaCl)	0.26	2.30	38.4	0.160	0.001	0.159	0.387	41.1
	0.52	4.70	19.1	0.174	0.004	0.170		43.9
	2.09	18.7	4.80	0.177	0.066	0.111		28.7

*P_{Theoric} = OCV_{Theoric} x Current, **Yield (%) = (P_{Net} / P_{Theoric}) x 100, OCV_{Theoric} data given in Figure 2a.

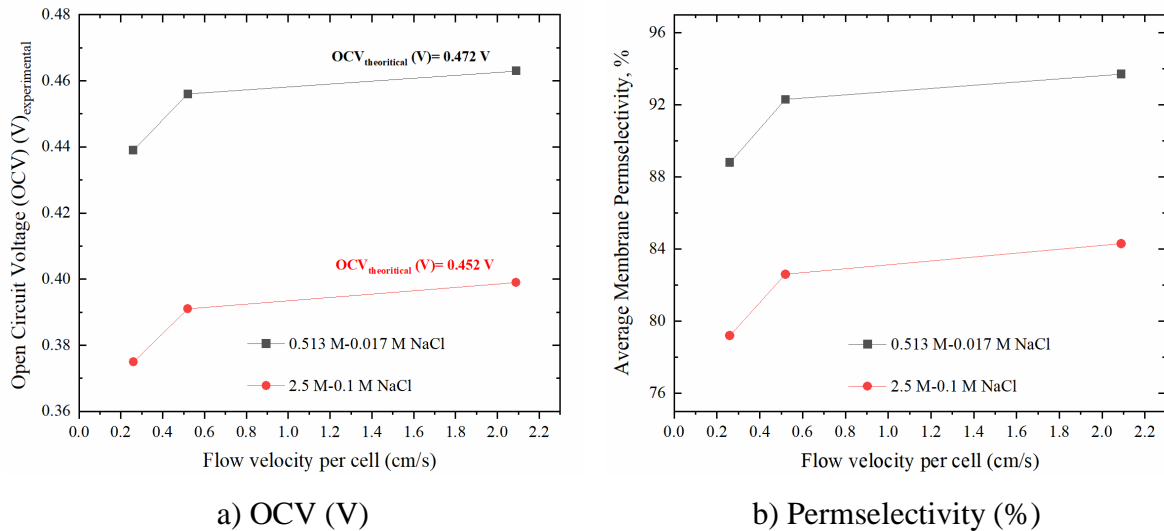


Figure 2. a) Experimental OCV (V), b) Average membrane permselectivity (%). Average membrane permselectivity was calculated as the ratio of experimental and theoretical OCV values ($OCV_{\text{experimental}}/OCV_{\text{theoretical}}$) (Theoretical OCV values were embedded in Figure 2a).

3.2. Effect of multivalent ion and flow velocity of electrolyte solution on RED performance

In real energy harvesting applications, monovalent and multivalent ions are present simultaneously in the feed electrolyte solutions [19-23]. Therefore, examining the multivalent ions' effect on the power generation performance is essential. In this section, the power densities of the RED system in the presence of divalent ions (SO_4^{2-}) were determined using different electrolyte solution concentrations and flow velocities. Table 4 indicates the power density and

P_{Net} values produced by the RED system and power loss (PL) when SO_4^{2-} are in different mole ratios in concentrate and dilute electrolyte solution compartments. The PL values in Table 4 show the power density difference of the RED system performed in the presence and absence of SO_4^{2-} ions.

The results indicated the power density increased as the flow velocity increased in all feed solution compositions, like the monovalent (Cl^-) ion study. However, it has been shown that the power density produced in the presence of SO_4^{2-} ions was lower compared with the presence of Cl^- ions (Table 3). These results indicate a decrease in generated power density when SO_4^{2-} ions are used. There are two fundamental reasons for the occurrence of PL. The first is the uphill transport created by the SO_4^{2-} ions since the membranes have low permselectivity against $\text{Cl}^-/\text{SO}_4^{2-}$ ions, and the second is the increasing membrane resistances in the presence of SO_4^{2-} ions. Further, the PL also varies depending on the SO_4^{2-} ion concentrations and the compartments in which it is used (Table 4). To this end, the effect of SO_4^{2-} ion concentration and the compartment composition on the PL was investigated by applying two different strategies in detail.

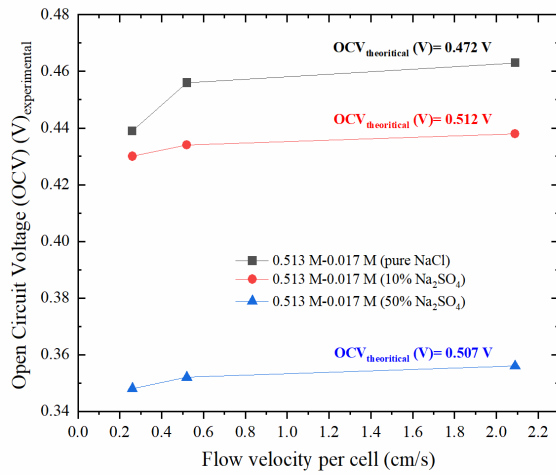
In the first strategy, the same amount of SO_4^{2-} ions was used in the dilute and concentrate compartments (Table 4). The results showed that increasing the amount of SO_4^{2-} ions from 10% mole to 50% mole in the total electrolyte solution decreased the power density dramatically and parallelly increased the PL. Pintossi et al. [20, 22] reported similar results and observed that power density decreased when the mole ratio of SO_4^{2-} ions increased in the feed electrolyte solution. These results can be explained by the three different transport: i) low permselectivity of AEMs ($\text{Cl}^-/\text{SO}_4^{2-}$), ii) reduced fixed charge group numbers in AEMs, and iii) increased membrane resistance. Increasing the multivalent ion concentrations in the feed electrolyte solution made these three transports more dominant, resulting in a heavy loss of power density. Figure 3 shows the theoretical and experimental OCV values and the average membrane permselectivity as a function of SO_4^{2-} ion concentrations using three different flow velocities. The difference between the theoretical and experimental OCV values shows a measure of total resistances formed on the membrane and $\text{Cl}^-/\text{SO}_4^{2-}$ permselectivity. Although the theoretical OCV value of the system when using the 50% mole of SO_4^{2-} ions in both compartments' solution was the highest, the experimental OCV values were the lowest at three different flow velocities. This means high SO_4^{2-} ion concentrations create more total resistances by decreasing membrane permselectivity, resulting in a loss of power density.

The second strategy used different SO_4^{2-} ion concentrations in the dilute and concentrate compartments to understand the compartment composition's effects on the RED performance. High ion concentration was first used in the dilute and then in the concentrate compartments (Table 4). The results showed that when the high SO_4^{2-} ion concentration was used in the dilute compartment, the power density values at three flow velocities decreased more than the low SO_4^{2-} ion concentration used in the same compartment. The reason is that electroneutrality is the dominant transport mechanism when using high SO_4^{2-} ion concentration in dilute compartments rather than the resistances. In summary, the PL results in Table 4 indicate divalent ions in the feed electrolyte solution cause heavy power density loss due to creating uphill transport, increasing total resistance, and decreasing membrane permselectivity.

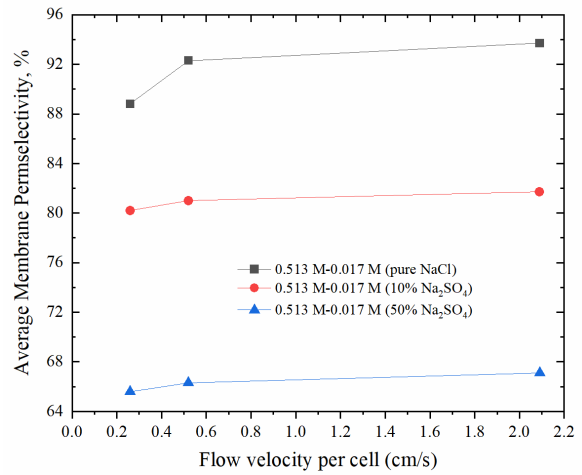
Table 4. The RED performance of Fujifilm Type II IEMs in the presence of multivalent ions.

Membranes	Flow velocity (cm/s)	Re	t_{res} (s)	Power density (W/m ²)	P_{pump} (W/m ²)	P_{Net} (W/m ²)	*PL (%)
0.017 M (90% NaCl+10% Na ₂ SO ₄) & 0.513 M (90% NaCl+10% Na ₂ SO ₄)	0.26	2.30	38.4	0.115	0.001	0.114	26.5
	0.52	4.70	19.1	0.142	0.004	0.138	19.3
	2.09	18.7	4.80	0.183	0.066	0.117	10.7
0.017 M (50% NaCl+50% Na ₂ SO ₄) & 0.513 M (50% NaCl+50% Na ₂ SO ₄)	0.26	2.30	38.4	0.085	0.001	0.084	45.8
	0.52	4.70	19.1	0.093	0.004	0.089	47.9
	2.09	18.7	4.80	0.111	0.066	0.045	65.6
0.017 M (50% NaCl+50% Na ₂ SO ₄) & 0.513 M (90% NaCl+10% Na ₂ SO ₄)	0.26	2.30	38.4	0.114	0.001	0.113	27.1
	0.52	4.70	19.1	0.116	0.004	0.111	35.1
	2.09	18.7	4.80	0.133	0.066	0.067	48.9
0.017 M (90% NaCl+10% Na ₂ SO ₄) & 0.513 M (50% NaCl+50% Na ₂ SO ₄)	0.26	2.30	38.4	0.122	0.001	0.121	22.0
	0.52	4.70	19.1	0.128	0.004	0.124	27.5
	2.09	18.7	4.80	0.152	0.066	0.086	34.4

*PL (%) = ((P_{NET})_{NaCl} - (P_{NET})_{NaCl+Na₂SO₄}) / (P_{NET})_{NaCl}, (P_{NET})_{NaCl} data given in Table 2.



a) OCV (V)



b) Permselectivity (%)

Figure 3. a) Experimental OCV (V), b) Average membrane permselectivity (%). Average membrane permselectivity was calculated as the ratio of experimental and theoretical OCV values ($OCV_{experimental}/OCV_{theoretical}$) (Theoretical OCV value was embedded in Figure 3a).

3.3. Organic fouling tendency and long-term performance of IEMs

The determination of the fouling behavior of membranes is of such importance for guiding real applications. It is well known that organic, inorganic, and biological substances are commonly present in natural water sources, and these substances play a significant role in membrane fouling, decreasing performance and shelf life and increasing operating costs [23]. In the scope of this study, the organic fouling behavior of AEMs was tested using a real (not model) humic and fulvic acid mixture solution. The main reason for examining the fouling behavior of AEMs is that their structures have a positive charge. Most of the substances in nature have a negative charge. Therefore, the electrostatic interactions between the negatively charged substances and positively charged AEMs surfaces become more dominant and trigger fouling exponentially. Since CEMs have a negative charge, electrostatic repulsion occurs between the contaminant and the membrane surface. Therefore, CEMs do not get fouled as much as AEMs. For this reason, there is a vigorous effort in the literature to produce fouling-resistant AEMs.

Figure 4 shows the P_{Net} values of the RED system before and after exposure of the AEMs to the humic and fulvic acid mixture solution. The maximum P_{Net} values were obtained at a current density of 8 A/m^2 for both conditions. However, a 30% decrease was observed in the maximum P_{Net} values after membrane fouling. This is because organic acid molecules are present in the membrane structure even after washing. Figure 5 shows AEM surface images before and after the fouling test. While the non-fouled membrane is white, the fouled membrane is yellow-brown. The color change refers to the presence of organic molecules in the membrane structure, decreasing the power generation performance of the RED system by reducing permselectivity and increasing resistances. Vital et al. [30] used natural water in reverse electrodialysis for energy generation and observed fouling on the membrane surface since the membrane color changed dramatically after the operation, like ours. Further, they applied the pre-treatment protocol to the feed water to mitigate the membrane fouling, and the results indicated the pre-treatment worked to prevent fouling. Similarly, Vermaas et al. [23] investigated the effect of natural seawater and river water for the feed electrolyte solution on the energy generation performance from the RED system with a long-term study. They reported that power density dropped approximately 40% at the end of the first day due to the organic fouling layers on the membrane structures.

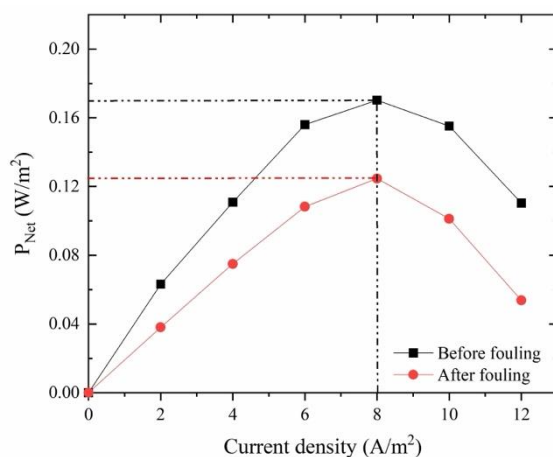


Figure 4. Effect of organic foulants on the power generation performance. (0.52 cm/s constant flow velocity and 0.017 M NaCl / 0.513 M NaCl electrolyte solution pair)

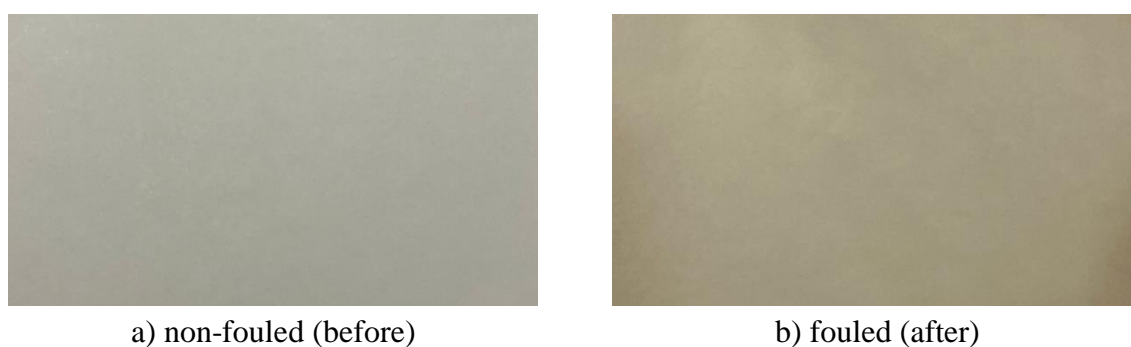


Figure 5. Membrane surface images a) before and b) after exposure to organic acid mixture.

Testing membranes' long-term performance is critical in determining their usability in industrial-scale systems. To this end, the RED system was operated for 4 hours nonstop with a constant current density of 8 A/m² and flow velocity of 0.52 cm/s with a 0.017 M NaCl / 0.513 M NaCl electrolyte solution pair. Figure 6 shows the RED system's long-term power generation performance. The result indicates that the initial P_{Net} value of the RED system where non-fouled membranes are used decreased gradually until 2 hours. Then, the value almost reached a stable and kept constant. The reason for the drop in performance in the first 2 hours is the accumulation of salt ions in the membrane structure over time. This means that fouling slowly occurred in the membrane structure. This period can be defined as the time required for the system to reach a steady state. On the other hand, the initial P_{Net} of the RED system where fouled membranes decreased sharply by almost 30%, and the value was constant during the operation. These obtained results show that membrane fouling significantly reduces the power generation performance of the RED system.

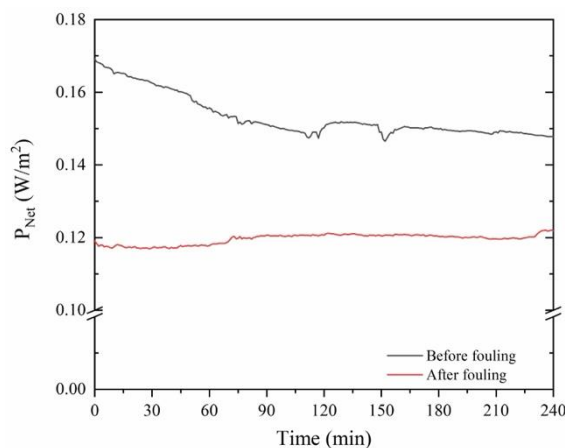


Figure 6. Long-term stability test of the RED system.

4. Conclusion

This study showed the effect of divalent ions, organic acids, electrolyte solution concentration, and flow velocity, significantly affecting the power generation performance in real applications. The flow velocity effect results indicated that the power generation performance decreased as the flow velocity reduced due to increased system resistances with decreasing flow velocity, especially non-ohmic resistances. The general projection for industrial-scale RED applications is to use sea and river water as feed electrolyte solutions. In this respect, the solution concentration pair used in this study, which corresponds to sea and river salinity, is of a nature that will shed light on industrial-scale studies. This study also indicated that divalent ions and organic substances seriously affected the power generation performance negatively. In particular, a significant drop in performance was observed as the concentration of divalent ions used in the compartments was increased. In addition, studies on the effect of composition in the compartments have shown that high divalent ion concentrations used in the dilute compartments have a more negative on performance. These results reveal that electrolyte solutions must be pretreated before feeding them to the RED system. In addition to the pretreatment protocol, coating the membrane surfaces with fouling-resistant materials, especially organic and biofouling, will reduce fouling and increase monovalent ion selectivity, increasing energy efficiency.

Ethics in Publishing

There are no ethical issues regarding the publication of this study.

Author Contributions

The author contributed to the study in terms of data curation, investigation, conceptualization, writing-original draft, funding acquisition, and project administration.

Acknowledgments

This study was supported by the Scientific and Technological Research Council of Turkey (TÜBİTAK) under the 2218 National Postdoc Project (Grant Number: 118C549). The author thanks TÜBİTAK for their support. I acknowledge FUJIFILM Manufacturing Europe BV for sending Fujifilm Type II IEMs and Assoc. Prof. Dr. Enver GÜLER for his effort in providing them. I want to acknowledge Prof. Dr. Nalan KABAY for providing me with all the equipment I need to use in my work.

References

- [1] Yip, N. Y., Brogioli, D., Hamelers, H. V. M., Nijmeijer, K. (2016) Salinity gradients for sustainable energy: primer, progress, and prospects. *Environmental Science & Technology*, 50 (22), 12072-12094.
- [2] Logan, B. E., Elimelech, M., (2012) Membrane-based processes for sustainable power generation using water. *Nature*, 488, 313-319.
- [3] Ramon, G. Z., Feinberg, B. J., Hoek, E. M. V. (2011) Membrane-based production of salinity gradient power. *Energy & Environmental Science*, 4, 4423-4434.
- [4] Weinstein, J. N., Leitz, F. B. (1976) Electric power from differences in salinity: the dialytic battery. *Science*, 191, 557-559.
- [5] Veerman, J., Saakes, M., Metz, S. J., Harmsen, G. J. (2010) Electrical power from sea and river water by reverse electrodialysis: a first step from the laboratory to a real power plant. *Environmental Science & Technology*, 44, 9207-9212.
- [6] Kuleszo, J., Kroeze, C., Post, J., Fekete, B. M. (2010) The potential of blue energy for reducing emissions of CO₂ and non-CO₂ greenhouse gases. *Journal of Integrative Environmental Sciences*, 7, 89-96.
- [7] Długołęcki, P., Antoine, G., Nijmeijer, K., Wessling, M. (2009) Practical potential of reverse electrodialysis as process for sustainable energy generation. *Environmental Science & Technology*, 43 (17), 6888-6894.
- [8] Tristan, C., Fallanza, M., Ibanez, R., Ortiz, I. (2020) Recovery of salinity gradient energy in desalination plants by reverse electrodialysis. *Desalination*, 496, 114699.
- [9] Tian, H., Wanga, Y., Peia, Y., Crittenden, J. C. (2020) Unique applications and improvements of reverse electrodialysis: A review and outlook. *Applied Energy*, 262, 114482-114506.
- [10] Audinos, R. (1983) Electrodialyse inverse. Etude de l'energie electrique obtenue a partir de deux solutions de salinites differentes. *Journal of Power Sources*, 10, 203-217.

- [11] Długolecki, P., Nijmeijer, K., Metz, S., Wessling, M. (2008) Current status of ion exchange membranes for power generation from salinity gradients. *Journal of Membrane Science*, 319, 214-222.
- [12] Veerman, J., de Jong, R. M., Saakes, M., Metz, S. J., Harmsen, G. J. (2009) Reverse electrodialysis: comparison of six commercial membrane pairs on the thermodynamic efficiency and power density. *Journal of Membrane Science*, 343, 7-15.
- [13] Długolecki, P., Ogonowski, P., Metz, S. J., Saakes, M., Nijmeijer, K., Wessling, M. (2010) On the resistances of membrane, diffusion boundary layer and double layer in ion exchange membrane transport. *Journal of Membrane Science*, 349, 369-379.
- [14] Veerman, J., Saakes, M., Metz, S. J., Harmsen, G. J. (2011) Reverse electrodialysis: a validated process model for design and optimization. *Chemical Engineering Journal*, 166, 256-268.
- [15] Vermaas, D. A., Saakes, M., Nijmeijer, K. (2011) Doubled power density from salinity gradients at reduced intermembrane distance. *Environmental Science & Technology*, 45, 7089-7095.
- [16] Burheim, O. S., Seland, F., Pharoah, J. G., Kjelstrup, S. (2012) Improved electrode systems for reverse electro-dialysis and electro-dialysis. *Desalination*, 285, 147-152.
- [17] Veerman, J., Saakes, M., Metz, S. J., Harmsen, G. J. (2010) Reverse electrodialysis: evaluation of suitable electrode systems. *Journal of Applied Electrochemistry*, 40, 1461-1474.
- [18] Vermaas, D. A., Bajracharya, S., Sales, B. B., Saakes, M., Hamelers, B., Nijmeijer, K. (2013) Clean energy generation using capacitive electrodes in reverse electrodialysis. *Energy & Environmental Science*, 6, 643-651.
- [19] Tedesco, M., Brauns, E., Cipollina, A., Micale, G., Modica, P., Russo, G., Helsen, J. (2015) Reverse electrodialysis with saline waters and concentrated brines: a laboratory investigation towards technology scale-up. *Journal of Membrane Science*, 492, 9-20.
- [20] Pintossi, D., Chen, C-L., Saakes, M., Nijmeijer, K., Borneman, Z. (2020) Influence of sulfate on anion exchange membranes in reverse electrodialysis. *npj Clean Water*, 3, 29.
- [21] Vermaas, D. A., Veerman, J., Saakes M., Nijmeijer, K. (2014) Influence of multivalent ions on renewable energy generation in reverse electrodialysis. *Energy & Environmental Science*, 7, 1434-1445.
- [22] Pintossi, D., Simoes, C., Saakes, M., Borneman, Z., Nijmeijer, K. (2021) Predicting reverse electrodialysis performance in the presence of divalent ions for renewable energy generation. *Energy Conversion and Management*, 243, 114369.
- [23] Vermaas, D. A., Kunteng, D., Saakes, M., Nijmeijer, K. (2013) Fouling in reverse electrodialysis under natural conditions. *Water Research*, 47, 1289-1298.

[24] <https://www.sefar.com/en/>, 01.10.2024.

[25] Jang, J., Kang, Y., Han, J. H., Jang, K., Kim, C. M., Kim, I. S. (2020) Developments and future prospects of reverse electrodialysis for salinity gradient power generation: Influence of ion exchange membranes and electrodes. *Desalination*, 491, 114540.

[26] Emdadi, A., Hestekin, J., Greenlee, L. F. (2021) Salt screening analysis for reverse electrodialysis. *Sustainable Energy & Fuels*, 5, 6135-6144.

[27] Golubenko, D. V., Van der Bruggen, B., Yaroslavtsev, A. B. (2021) Ion exchange membranes based on radiation-induced grafted functionalized polystyrene for high-performance reverse electrodialysis. *Journal of Power Sources*, 511, 230460.

[28] Vermaas, D. A., Guler, E., Saakes, M., Nijmeijer, K. (2012) Theoretical power density from salinity gradients using reverse electrodialysis. *Energy Procedia*, 20, 170-184.

[29] Altıok, E., Kaya, T. Z., Güler, E., Kabay, N., Bryjak, M. (2021) Performance of reverse electrodialysis system for salinity gradient energy generation by using a commercial ion exchange membrane pair with homogeneous bulk structure. *Water*, 13, 814.

[30] Vital, B., Torres, E. V., Sleutels, T., Gagliano, M. C., Saakes, M., Hamelers, H. V. M. (2021) Fouling fractionation in reverse electrodialysis with natural feed waters demonstrates dual media rapid filtration as an effective pre-treatment for fresh water. *Desalination*, 518, 115277.